The Role of Inelastic Electron-Phonon Interaction on the On-Current and Gate Delay Time of CNT-FETs

M. Pourfath, H. Kosina, and S. Selberherr
Institute for Microelectronics, TU Wien, Gußhausstraße 27–29/E360, 1040 Wien, Austria
Phone: +43-1-58801/36031, Fax: +43-1-58801/36099, Email: pourfath@iue.tuwien.ac.at

***Abstract*— The performance of carbon nanotube field-effect transistors is analyzed using the non-equilibrium Green's function formalism. The role of the inelastic electron-phonon interaction on both, on-current and gate delay time, is studied. For the calculation of the gate delay time the quasi-static approximation is assumed. The results confirm experimental data of carbon nanotube transistors, where the on-current can be close to the ballistic limit, but the gate delay time can be far below that limit.**

I. Introduction

Carbon nanotube field-effect transistors (CNT-FETs) have been considered in recent years as potential alternatives to CMOS devices. A CNT can be viewed as a rolled-up sheet of graphene with a diameter of a few nano-meters. The way the graphene sheet is wrapped is represented by a pair of indices (n, m) called the chiral vector. The integers n and m denote the number of basis vectors along two directions in the honeycomb crystal lattice of graphene. The CNT is called *zigzag*, if $m = 0$, *armchair*, if $n = m$, and *chiral* otherwise. CNTs with $\mathrm{n} - \mathrm{m} = 3$ are metals, otherwise they are semiconductors. Semiconducting CNTs can be used as channels for transistors which have been studied in recent years.

Depending on the work function difference between the metal contact and the CNT, carriers at the metal-CNT interface encounter different barrier heights (see Fig. 1). Fabrication of devices with positive (Schottky type) [1] and zero (Ohmic) [2] barrier heights for holes have been reported. In this work we consider devices with zero barrier heights for electrons.

The non-equilibrium Green's function (NEGF) method has been successfully utilized to investigate the characteristics of nano-scale silicon transistors [3], CNT-FETs [4], and molecular devices [5]. To extend our previous works [6, 7], the NEGF formalism is employed to study the effect of inelastic electron-phonon interaction on the on-current and gate delay time of CNT-FETs in more detail.

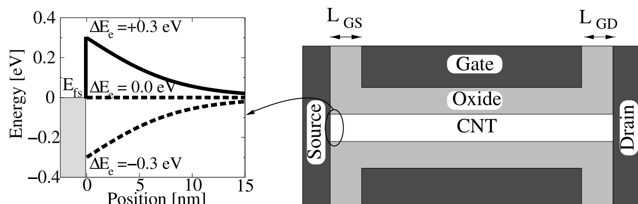

Fig. 1: Sketch of the CNT-FET investigated. The insulating layer is $\mathrm{HfO_2}$ with $\epsilon_\mathrm{r} = 20$ and a thickness of 2 nm. The geometry parameters are L_GS=L_GD=4 nm and $L_\mathrm{CNT} = 50$ nm.

II. Approach

Using the NEGF formalism quantum phenomena like tunneling, and scattering processes can be rigorously modeled [8]. Based on the NEGF formalism we investigated the effect of the electron-phonon interaction on the performance of CNT-FETs.

The transport equations are solved on the surface of the CNT. Due to quantum confinement along the tube circumference, the wave-functions of carriers are bound around the CNT and can propagate along the tube axis. We considered an azimuthal symmetric structure, in which the gate fully surrounds the CNT. Under the assumption that the potential profile does not vary sharply along the CNT, sub-bands are decoupled [9]. As a result, transport equations need to be solved only along the CNT axis which is assumed to be the z direction in cylindrical coordinates. In this work we assume bias conditions for which the first sub-band contributes mostly to the total current. In the mode-space approach the transport equation for a sub-band can be written as [4]

$$G^{\mathrm{r,a}}_{\mathbf{r},\mathbf{r}'}(E) = [EI - H_{\mathbf{r},\mathbf{r}'}(E) - \Sigma^{\mathrm{r,a}}_{\mathbf{r},\mathbf{r}'}(E)]^{-1} \tag{1}$$

$$G^{\gtrless}_{\mathbf{r},\mathbf{r}'}(E) = G^{\mathrm{r}}_{\mathbf{r},\mathbf{r}'}(E)\Sigma^{\gtrless}_{\mathbf{r},\mathbf{r}'}(E)G^{\mathrm{a}}_{\mathbf{r},\mathbf{r}'}(E) \tag{2}$$

In (1) an effective mass Hamiltonian was assumed. All our calculations assume a CNT with a band gap of $\mathrm{E_g} = 0.6$ eV corresponding to a CNT with a diameter of $\mathrm{d_{CNT}} = 1.6$ nm, and $m^* = 0.05m_0$ for both electrons and holes. A recursive Green's function method is used for solving (1) and (2) [3].

Using a perturbation expansion one can define the self-energy Σ as an irreducible part of the Green's function. An exact evaluation of the self-energy is possible only for some rather pathological models. For real systems one has to rely on approximation schemes. The total self-energy in (1) consists of the self-energies due to the source contact, drain contact, and electron-phonon interaction, $\Sigma^r = \Sigma^r_\mathrm{S} + \Sigma^r_\mathrm{D} + \Sigma^r_\mathrm{e-ph}$. In order to solve the system of equations in a finite system, boundary conditions have to be specified. The boundary conditions of (1) have to model the contacts which act as a source or drain for electrons and can be imposed by adding self-energies. These are non-zero only at the boundaries and can be calculated as [4].

In this work the first-order self-energy for electron-phonon interaction within the self-consistent Born approximation is applied [10]. The interaction of electrons with optical phonons is inelastic. Assuming that the electron-phonon interaction

1-4244-1124-6/07/$25.00 ©2007 IEEE.

occurs locally, $\Sigma_{\mathbf{r},\mathbf{r}'}(E) = 0$ [11] for $\mathbf{r} \neq \mathbf{r}'$, the self-energy for inelastic electron-phonon interaction can be written as

$$\Sigma^{<}_{\mathrm{e-ph}}(E) = \sum_{\lambda} D_{\lambda}(n_B(\hbar\omega_{\lambda}) + \frac{1}{2} \pm \frac{1}{2})G^{<}(E \pm \hbar\omega_{\lambda}) \quad (3)$$

where $\hbar\omega_{\lambda}$ denotes the phonon energy of branch λ, $n(\hbar\omega_{\lambda})$ the average phonon occupation number, and D_{λ} the electron-phonon coupling strength. The plus and minus signs in (3) denote the phonon emission and absorption processes, respectively. Assuming that the bath of phonons is maintained in thermodynamic equilibrium, $n(\hbar\omega_{\lambda})$ is given by the Bose-Einstein distribution function. The electron-phonon interaction strength of a $(n, 0)$ zigzag CNT is given by

$$D_{\lambda} = \frac{\hbar|M_{\lambda}|^2}{2nm_{\mathrm{c}}\omega_{\lambda}} , \quad (4)$$

where the matrix elements of the interaction Hamiltonian M_{λ} depend on the diameter and the chirality of the CNT. The calculation of these parameters is presented in [12, 13]. Phonons with $\mathbf{q} \approx 0$ are referred to as Γ-point phonons, and can belong to the twisting acoustic (TW), the longitudinal acoustic (LA), the radial breathing mode (RBM), the out-of-phase out-of-plane optical (ZO), the transverse optical (TO), or the longitudinal optical (LO) phonon branch. Phonons inducing inter-valley transitions have a wave-vector of $|\mathbf{q}| \approx q_{\mathrm{K}}$, where q_{K} corresponds to the wave-vector of the K-point of the Brillouin zone of graphene. K-point phonons, also referred to as zone boundary phonons, are a mixture of fundamental polarizations.

The greater self-energy is calculated similar to (3) and the retarded self-energy is given by

$$\Sigma^{\mathrm{r}}_{\mathrm{e-ph}}(E) = -\frac{i}{2}\Gamma_{\mathrm{e-ph}}(E) + \mathrm{P}\int \frac{dE'}{2\pi}\frac{\Gamma_{\mathrm{e-ph}}(E')}{E - E'} , \quad (5)$$

where $\Gamma_{\mathrm{e-ph}} \equiv i(\Sigma^{>}_{\mathrm{e-ph}} - \Sigma^{<}_{\mathrm{e-ph}})$ defines the broadening, and $\mathrm{P}\int$ represents the principal part of the integration. The imaginary part of the retarded self-energy broadens the density of states, whereas the real part shifts it in energy.

The transport equations (1) and (2) are iterated to achieve convergence of the electron-phonon self-energies, resulting in a self-consistent Born approximation. Then the coupled system of transport and Poisson equation is solved iteratively. To solve the transport equations numerically, they need to be discretized in both the spatial and the energy domain. Uniform spatial grids have been employed. The carrier concentration at some node l and the current density between the nodes l and $l+1$ of the device are given by

$$n_l = -4i\int \frac{dE}{2\pi}G^{<}_{l,l}(E) , \quad (6)$$

$$j_{l,l+1} = \frac{4\mathrm{q}}{\hbar}\int \frac{dE}{2\pi}2\Re e\{G^{<}_{l,l+1}(E)H_{l+1,l}\} , \quad (7)$$

where the factor 4 is due to the spin and band degeneracy. In the Poisson equation carriers are treated as a sheet charge distributed over the surface of the CNT [14, 15]. The energy grid, however, has to be non-uniform, since an adaptive integration method is generally required to evaluate quantities such as (6) with sufficient accuracy.

The coupled system of the transport and Poisson equations has to be solved self-consistently [5], where the convergence of the self-consistent iteration is a critical issue. To achieve convergence, fine resonances at some energies in (6) have to be resolved accurately [15]. For that purpose an adaptive method for selecting the energy grid is essential [16].

III. The Effect of the Electron-Phonon Interaction on the On-Current

Fig. 2 shows the dependence of the ballisticity on the phonon energy. The ballisticity is defined as $I_{\mathrm{Sc}}/I_{\mathrm{Bl}}$, the ratio of the on-current in the presence of electron-phonon interaction to the current in the ballistic case [17]. With increasing phonon energy ballisticity increases. The left part of Fig. 3 illustrates an electron losing its kinetic energy by emitting a phonon. The electron will be scattered either forward or backward. In the case of backward scattering the electron faces a thick barrier near the source contact and will be reflected with high probability, such that its momentum will again be directed towards the drain contact. With increasing phonon energy the effect of phonon scattering on the current is reduced, because scattered electrons lose more kinetic energy and the probability for traveling back to the source contact decreases.

The considerable decrease of ballisticity for low energy phonons is due to the phonon absorption process. The right part of Fig. 3 shows an electron absorbing energy from a phonon and scattering into a higher energy state. In this case, the probability for arriving at the source contact increases. This process can severely reduce the total current. As the phonon energy decreases, the phonon occupation number increases exponentially, and the contribution of both phonon emission and absorption processes increases. However, due to the higher probability for back-scattering of electrons in the case of

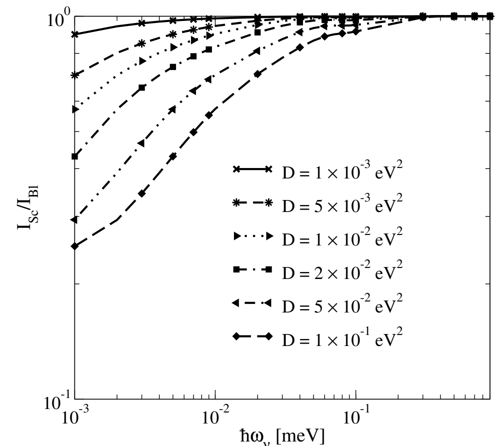

Fig. 2: Ballisticity versus phonon energy for a CNT of 50 nm length. Results for inelastic scattering with different electron-phonon couplings are shown for $V_{\mathrm{G}} = V_{\mathrm{D}} = 1$ V.

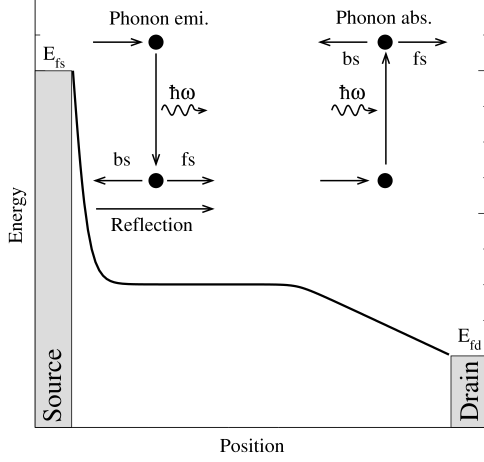

Fig. 3: Sketch of phonon emission and absorption processes in the channel.

phonon absorption, this component reduces the total current more effectively than the phonon emission process does.

IV. The Effect of the Electron-Phonon Interaction on the Gate Delay Time

To investigate the dynamic response of the device we consider the gate delay time defined as:

$$\tau = \frac{C_{\mathrm{G}} V_{\mathrm{DD}}}{I_{\mathrm{on}}} \tag{8}$$

Here, $C_{\mathrm{G}} = C_{\mathrm{Ins}}{}^{-1} + C_{\mathrm{Q}}{}^{-1}$. The quantum capacitance is given by $C_{\mathrm{Q}} = 8\mathrm{q}^2/\mathrm{h}\upsilon_{\mathrm{F}} \approx 400\mathrm{aF}/\mu\mathrm{m}$, including the twofold band and spin degeneracy. If thin and high-κ insulators are used, then $C_{\mathrm{Ins}} \gg C_{\mathrm{Q}}$ and $C_{\mathrm{G}} \approx C_{Q}$, implying that the potential on the tube becomes equal to the gate potential (perfect coupling). This regime is called quantum capacitance limit in which the device is potential-controlled rather than charge-controlled [18]. The insulator capacitance, occurring between the tube and a cylindrical gate, is given by

$$C_{\mathrm{Ins}} = \frac{2\pi\kappa\epsilon_0}{\ln(T_{\mathrm{Ins}}/R_{\mathrm{CNT}} + 1)} \tag{9}$$

For the geometry parameters given in Fig. 1 $C_{\mathrm{Ins}} \approx 1500\mathrm{aF}/\mu\mathrm{m}$, satisfying the condition of the quantum capacitance limit [19] ($C_{\mathrm{Q}} \ll C_{\mathrm{Ins}}$). Therefore, one gets $C_{\mathrm{G}} V_D \approx Q_{\mathrm{Ch}}$, where Q_{Ch} is the total charge in the CNT channel. The gate delay time can be written as $\tau \approx Q_{\mathrm{Ch}}/I_{\mathrm{D}}$. Here, the quasi-static approximation is assumed. It has been shown that for CNT based transistors this approximation is justified for frequencies below THz [20].

Fig. 4 shows the ratio of the gate delay time in the presence of electron-phonon interaction to that in the ballistic case, $\tau_{\mathrm{Sc}}/\tau_{\mathrm{Bl}}$, as a function of the electron-phonon coupling strength. As the phonon energy increases the gate delay time increases. This behavior can be attributed to the electron group velocity in the channel, which is high for ballistic electrons and low for electrons scattered to lower energy states. Fig. 5 shows the spectra of the source and drain currents

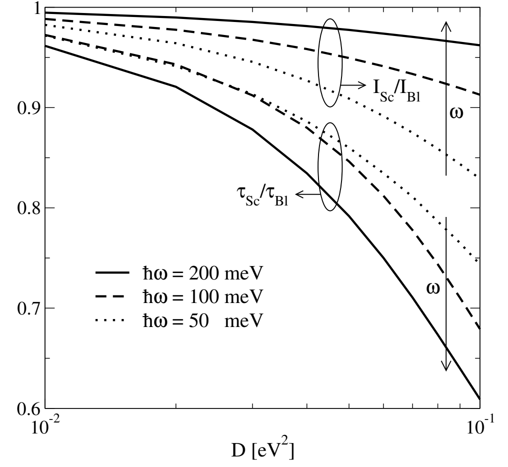

Fig. 4: The ratio of the gate delay time in the presence of electron-phonon interaction to that in the ballistic case, $\tau_{\mathrm{Sc}}/\tau_{\mathrm{Bl}}$, as a function of the electron-phonon coupling strength. For comparison, the ratio $I_{\mathrm{Sc}}/I_{\mathrm{Bl}}$ is also shown. As the phonon energy increases the gate delay time increases.

for different phonon energies. Electrons can emit a single phonon or a couple of phonons to reach lower energy states. The probability of n sequential electron-phonon interactions decreases as n increases. Therefore, as the phonon energy increases, the occupation of electrons at lower energy states increases. Fig. 5 shows a considerable increase of the electron population close to the conduction band-edge as the phonon energy increases. Therefore, the mean velocity of electrons decreases and the carrier concentration in the channel increases (Fig. 6). The increased charge in the channel results in an increased gate delay time.

V. Discussion

Considering the CNTs with diameters in the range $d_{\mathrm{CNT}} = 1-2$ nm, the energies of important inelas-

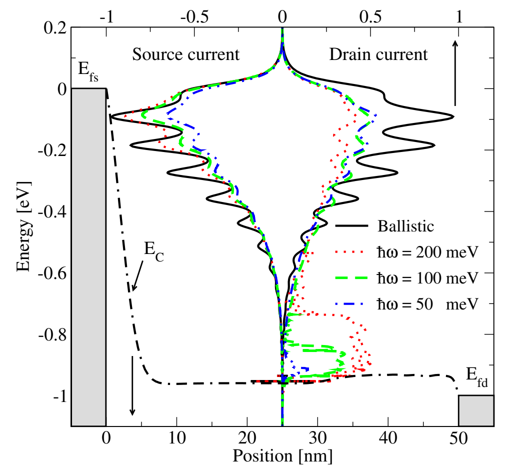

Fig. 5: The spectra of the source and drain currents. The effect of inelastic scattering with different phonon energies is shown. The electron-phonon coupling strength is $D = 2 \times 10^{-1}$ eV^2. The figure shows a considerable increase of the electron population close to the conduction band-edge as the phonon energy increases.

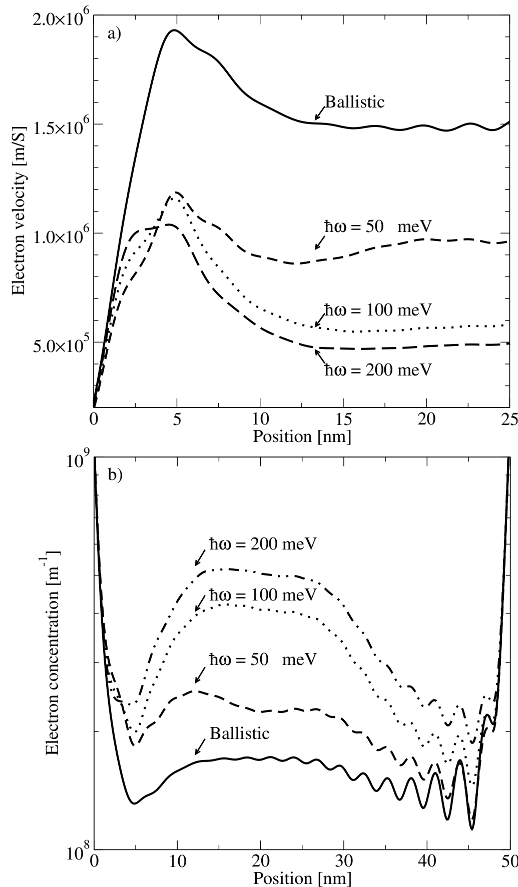

Fig. 6: a) The profile of the electron velocity near the source contact. b) The profile of the electron concentration along the device. The results for the ballistic case and for electron-phonon interaction are shown. As the phonon energy increases the electrons scatter to lower energy states. Therefore, the electron velocity decreases and the carrier concentration increases. The electron-phonon coupling strength is $D = 10^{-1}$ eV^2 and the bias point $V_{\rm G} = V_{\rm D} = 1$ V.

tic phonons are $\hbar\omega_{\rm OP} \approx 200$ meV, $\hbar\omega_{\rm RBM} \approx 30$ meV, and $\hbar\omega_{\rm K} \approx 160$ and 180 meV [17,21]. The corresponding coupling coefficients are $D_{\rm OP} \approx 40 \times 10^{-3}$ eV^2, $D_{\rm RBM} \approx 10^{-3}$ eV^2, and $D_{\rm K} \approx 10^{-4}$ and 50×10^{-3} eV^2 [12,17].

As discussed, high energy phonons such as OP and K-point phonons reduce the on-current only weakly, but can increase the gate delay time considerably due to charge pileup in the channel. Low energy phonons such as the RBM phonon can reduce the on-current more effectively, but have a weaker effect on the gate delay time. However, due to strong coupling, scattering processes are mostly due to electron-phonon interaction with high energy phonons. Therefore, the on-current of short CNT-FETs can be close to the ballistic limit [22] (see Fig. 7), whereas the gate-delay time can be significantly below that limit.

The gate delay time for the ballistic case can be approximated as $\tau \approx 1.7$ ps$/\mu$m, or equivalently $f_T \approx 100$ GHz$/\mu$m [23]. The highest reported cut-off frequency for a device with a length of less than 1μm is $f_T \approx 10$ GHz [24], which is far below the ballistic limit. Apart from parasitic capacitances, inelastic electron-phonon interaction with high energy phonon has to be considered to explain the results.

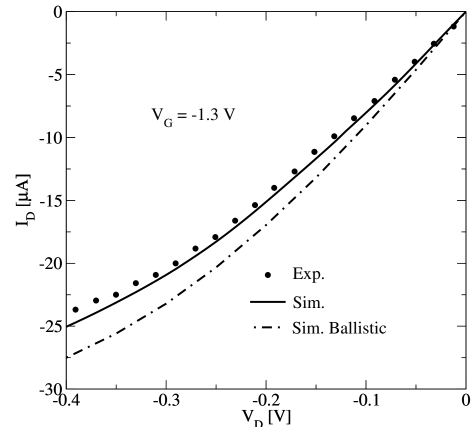

Fig. 7: Comparison of the simulation results and experimental data [22] for the output characteristics. The results for the bias point $V_{\rm G} = -1.3$ V are compared with the ballistic limit.

VI. Conclusion

The effect of the electron-phonon interaction parameters on the performance of CNT based transistors was studied, using the NEGF formalism. Inelastic scattering with high energy phonons reduces the on-current only weakly, whereas it can increase the gate delay time considerably. The results explain the reason why the measured on-currents of short CNT-FETs can be close to the ballistic limit, whereas the highest achieved cutoff frequency is significantly below that limit.

Acknowledgment

This work, as part of the European Science Foundation EUROCORES Programme FoNE, was supported by funds from FWF, CNR, EPSRC and the EC Sixth Framework Programme, under Contract N. ERAS-CT-2003-980409.

References

[1] J. Appenzeller *et al.*, Phys.Rev.Lett. **92**, 048301 (2004).
[2] A. Javey *et al.*, Letters to Nature **424**, 654 (2003).
[3] A. Svizhenko *et al.*, J.Appl.Phys. **91**, 2343 (2002).
[4] A. Svizhenko *et al.*, Phys.Rev.B **72**, 085430 (2005).
[5] F. Zahid *et al.*, Phys.Rev.B **70**, 245317 (2004).
[6] M. Pourfath *et al.*, in *ESSDERC Proc.* 210 (2006)
[7] M. Pourfath *et al.*, in *IEDM Tech.Dig.* 31.5.1 (2006)
[8] M. Pourfath *et al.*, IOP Journal of Physics: Conference Series **38**, 29 (2006).
[9] R. Venugopal *et al.*, J.Appl.Phys. **92**, 3730 (2002).
[10] R. Lake *et al.*, J.Appl.Phys. **81**, 7845 (1997).
[11] R. Lake *et al.*, Phys.Rev.B **45**, 6670 (1992).
[12] G. Mahan, Phys.Rev.B **68**, 125409 (2003).
[13] V. N. Popov *et al.*, Phys.Rev.B **74**, 075415 (2006).
[14] M. Pourfath *et al.*, Microelectronic Engineering **81**, 428 (2005).
[15] D. John *et al.*, in *Proc. NSTI Nanotech* **3**, 65 (2004)
[16] M. Pourfath *et al.*, Lecture Notes in Computer Science **3743**, 578 (2006).
[17] S. O. Koswatta *et al.*, Appl.Phys.Lett. **89**, 023125 (2006).
[18] J. Guo *et al.*, in *IEDM Tech.Dig.* 711 (2002)
[19] D. John *et al.*, J.Appl.Phys. **96**, 5180 (2004).
[20] Y. Chen *et al.*, Appl.Phys.Lett. **89**, 203122 (2006).
[21] J. Park *et al.*, Nano Lett. **4**, 517 (2004).
[22] A. Javey *et al.*, Nano Lett. **4**, 1319 (2004).
[23] Y. Yoon *et al.*, IEEE Trans. Electron Devices **53**, 2467 (2006).
[24] X. Huo *et al.*, in *IEDM Tech.Dig.* 691 (2004)